Measurement of the pulmonary vascular granulocyte pool

WLADIMIR Y. USSOV, A. MICHAEL PETERS, DAPHNE M. GLASS, RANJAN D. GUNASEKERA, AND J. MICHAEL B. HUGHES
Departments of Radiology and Medicine, Royal Postgraduate Medical School, Hammersmith Hospital, London W12 0HS, United Kingdom

Ussov, Wladimir Y., A. Michael Peters, Daphne M. Glass, Ranjan D. Gunasekera, and J. Michael B. Hughes. Measurement of the pulmonary vascular granulocyte pool. *J. Appl. Physiol.* 78(4): 1388–1395, 1995.—We have developed a technique for measuring the pulmonary granulocyte pool (PGP) as a fraction of the whole body total blood granulocyte pool (TBGP). The technique "captures" a dose of ^{99m}Tc-labeled granulocytes in a region of interest (ROI) over the lung during first pass by integrating an input time-activity curve from an ROI over the pulmonary artery, superior vena cava, or right ventricle. The ratio of the estimated first-pass count rate and the count rate in the same lung ROI after equilibration of the cells between the circulating and pulmonary pools (15–30 min) represents the PGP/TBGP. The technique was validated in eight subjects by using ^{99m}Tc-labeled macroaggregated human serum albumin. With corrections for background and injected doses, the ratios of first-pass granulocyte-to-macroaggregated human serum albumin count rates given by the three input ROIs were close to unity [superior vena cava 0.98 ± 0.079 (SD), right ventricle 1.01 ± 0.070, and pulmonary artery 0.97 ± 0.073]. Significant increases in PGP/TBGP were demonstrated in systemic inflammation. Thus, in patients with inflammatory bowel disease, it was 0.22 ± 0.07 (n = 7) compared with 0.08 ± 0.01 (n = 5) in control subjects. It was also elevated in patients with systemic vasculitis (0.34 ± 0.07; n = 5), in transplant recipients (0.33 ± 0.08; n = 5), and in patients with osteomyelitis (0.15 ± 0.06; n = 4). We conclude that this is a valid technique for quantifying the PGP that is expanded in several conditions associated with systemic inflammation.

^{99m}technetium-labeled granulocytes; lung vascular granulocyte pool; granulocyte kinetics

THROUGHOUT THE BODY, granulocytes are dynamically distributed between two pools: *1*) the marginating granulocyte pool, which is conceptually a population of cells slowly rolling along endothelial surfaces or at least delayed in their transit through a vascular bed, and *2*) the circulating granulocyte pool (CGP), which consists of cells in the axial stream of blood vessels passing through a vascular bed at the same speed as red blood cells. The two pools together make up the total blood granulocyte pool (TBGP). The CGP, marginated pool, and TBGP may be applied to whole body or regional pools. For instance, in the spleen, the marginated granulocyte pool appears to represent ~90% of the splenic TBGP (35), which itself makes up ~20–30% of the whole body TBGP. Margination is also probably high in the liver and, to a lesser extent, in the bone marrow. As far as the lung is concerned, the size of the pulmonary fraction of the whole body TBGP [from now on called the pulmonary granulocyte pool (PGP)] is controversial. We have previously suggested that the PGP is ~10% of the whole body TBGP or 25% of the whole body CGP (34), but others have suggested that it is much higher (18).

A major reason for an increasing interest in granulocyte traffic through the pulmonary vascular bed (25) is that granulocytes have been implicated in the pathogenesis of acute and chronic lung diseases (40), as well as in respiratory disorders associated with extensive extrapulmonary inflammation, including sepsis (47, 48), vasculitis (21), and peritonitis (13). Increased pulmonary vascular trapping of granulocytes may be a prerequisite for later extravascular migration, which itself is thought to play a role in damage to lung tissue in a wide range of pathological conditions (18).

To study pulmonary granulocyte kinetics, it is clearly necessary to have a technique for quantifying the PGP. This has previously been attempted in humans *1*) by expressing mean pulmonary granulocyte transit time as a quotient of the red blood cell transit time (29, 30, 34), *2*) by measuring granulocyte transit time in absolute time units (24, 29) during first pass through the lung after injection, *3*) as the ratio of chest to whole body radioactivity (4), *4*) as the half-time of clearance of radioactivity from the lung after injection (14), and *5*) semiquantitatively as the lung-to-liver ratio on early images after injection (20) or as the count rate per pixel of lung regions of interest (ROIs) per megabecquerel of injected ^{111}In (4). All of these approaches have relative drawbacks: expressing granulocyte transit time as a quotient of red blood cell transit time requires the injection of labeled red blood cells, the first-pass transit time may be influenced by the activity of in vitro manipulation [the "collection" injury (37)], and the other methods are semiquantitative. Furthermore, these techniques do not clearly separate the PGP into its circulating and marginating components, except in the comparison with red blood cell transit time where the quotient represents the "excess" of granulocytes (i.e., the regional marginated granulocyte pool) in the lung over the circulating component (34). Nevertheless, the use of the term "margination" in the lung should not be taken to imply a specific mechanism of trapping, and it may be more appropriate to consider the regional PGP as representing a continuous spectrum of granulocyte transit times through the lung (18, 25) rather than in terms of two discrete components.

In the current study, we have developed a new method for quantifying the PGP, without a separation into circulating and marginating components, using a technique based on the first pass of ^{99m}Tc-hexamethylpropyleneamine oxime-labeled granulocytes through the pulmonary vascular bed. In principle, the technique attempts to "encapsulate" the entire dose of labeled cells as it transits the lungs for the first time. An important advantage is that it does not assume that the first-pass transit time is identical to the times of transit

on subsequent passes. The later count rate at any time represents the PGP as a fraction of TBGP. In addition, by knowing the labeled granulocyte recovery at this time, this fraction can be converted to the fraction PGP/CGP, where CGP is the whole body circulating granulocyte pool. The aim of this study was to validate this technique and illustrate its application in several diseases in which abnormalities of pulmonary vascular traffic have previously been suggested (11, 20).

MATERIALS AND METHODS

Theory

The aim of the theory is to quantify the PGP as fractions of both the whole body TBGP and the whole body CGP. The principle of the technique is to "capture" the entire dose of ^{99m}Tc-labeled granulocytes in the lungs as they transit the lungs on first pass. The count rate (N_t) in an ROI over the lung at any subsequent time (t) expressed as a fraction of the first-pass count rate in the same ROI (N_1) will be equal to the ratio of the PGP expressed as a fraction of the whole body TBGP, i.e., PGP/TBGP = N_t/N_1, provided that no cells are irretrievably lost from the TBGP and that the cells have equilibrated throughout the marginating pools of the body by *time t*.

By taking a blood sample at *time t*, labeled granulocyte recovery [R(t); the fraction of labeled cells in the CGP] can be calculated. Provided equilibrium between the PGP and CGP is achieved when the lung ROI counts at *time t* are recorded, N_1 multiplied by R(t) represents the cells available to the pulmonary vasculature, and so the count rate at *time t* in the lung ROI represents the PGP as a fraction of the whole body CGP, i.e., PGP/CGP = $(N_t/N_1) \times (1/R)$. These equations further assume that *1*) all the cells are temporarily trapped in the lung on the first pass and *2*) that the fraction of the pulmonary arterial blood flow delivered to the lung ROI is equal to the fraction of the PGP in the ROI.

The first assumption above, that all the cells are briefly trapped in the lung on the first pass, was addressed by a technique that has previously been applied to the kidney for the measurement of renal blood flow and that, in the present study, uses the first-pass time-activity curve and a pulmonary arterial input curve derived from ROIs over the superior vena cava, right ventricle, or pulmonary artery as follows. The first-pass time-activity curves derived from ROIs over the superior vena cava, right ventricle, and pulmonary artery were corrected for recirculation and integrated. The integrated curves were then scaled to be parallel to the lung curve, whereupon each gives an independent estimate of the plateau that the lung curve would have reached if all the labeled granulocytes arriving in the lung were irreversibly trapped. This approach is similar in principle to the measurement of organ blood flow in which a scaled integrated recirculation-corrected curve obtained over the lung, left ventricle, or aorta is used to estimate the organ first-pass curve that would be obtained if an intravenously injected recirculating tracer had infinite transit time through the vasculature of the organ (31, 32).

As with organ blood flow, the scaling factor by which the integrated input curve is made parallel to the lung is equal to the ratio of the maximum slope of the lung curve (gL) to the maximum slope of the integrated input curve (gA). These slopes were obtained by an objective computerized technique (**Fig. 1**). The gradients gA and gL were estimated from a standard least squares fit to the upslope segments, comprising six or seven points, of the respective time-activity curves. The integrated input curve was then scaled by a factor equal to gL/gA so that the ratio of the resulting upslope gradients (i.e., of the integrated input curve and the lung curve) was equal to unity. In addition, we varied the scaling factor manually to obtain a value that visually appears to make the two curves parallel (Fig. 2). We then compared the maximum N_1 values given by the operator-independent and operator-dependent approaches.

This approach was validated in a separate group of eight subjects by comparing the plateau of the integrated granulocyte first-pass time-activity curve with the count rate in the same ROI obtained after an injection of a radiopharmaceutical that is physically 100% trapped in the lung vasculature and therefore has infinite pulmonary transit time, i.e., ^{99m}Tc-labeled macroaggregated human serum albumin (^{99m}Tc-MAA). Thus ^{99m}Tc-MAA was injected into the same patient before the labeled granulocytes, and the ratio of their respective count rates recorded in the same lung ROI (after correction of the signal from the cells for the preceding ^{99m}Tc-MAA) was compared with the ratio of their respective injected doses (measured in vitro).

The second assumption above, that the regional distributions of the PGP and pulmonary blood flow are comparable, may not be valid if, in the upper zones for example, the regional blood flow and regional PGP were not equal fractions of the whole lung values. To test this assumption, we compared the count rates in profiles over the right lung from base to apex on the ^{99m}Tc-MAA and the 15-min ^{99m}Tc-granulocyte image (corrected for the preceding ^{99m}Tc-MAA injection) in the same eight subjects.

Patients

Of the eight patients given ^{99m}Tc-MAA and labeled granulocytes for validation of the above assumptions, two were referred for suspected osteomyelitis (but had negative scans); four had a clinical diagnosis of inflammatory bowel disease (IBD), two of whom had intense accumulation of granulocytes in the bowel; and two, suspected of IBD, had a clinical report unequivocally negative for active IBD.

In 26 further patients, PGP was measured as a fraction of TBGP. These included five patients who were referred from the Department of Surgery (Orthopedics) for suspected osteomyelitis with a painful hip prosthesis or knee prosthesis. None gave a history of pyrexia during the month preceding referral. At the time of the study, each remained apyrexial and had a C-reactive protein level <8.5 mg/l, a white blood cell count $<9.1 \times 10^{12}$ cells/l with neutrophils $<6.8 \times 10^{12}$ cells/l, an erythrocyte sedimentation rate in the normal Westergren age-related range, and a negative granulocyte scan. The affected joint was considered noninfected on clinical follow-up of up to 4 mo. We therefore considered these five patients as showing no evidence of systemic inflammatory disease and used them as control subjects. Seven patients were referred with IBD (four with ulcerative colitis and three with Crohn's disease). All of them had abnormal ^{99m}Tc-granulocyte scans, indicative of active disease. Five other patients had systemic vasculitis: two were suspected of the enteric form of graft vs. host disease after bone marrow transplantation, two were referred with pyrexia of unknown origin after renal transplantation, and one with pyrexia of unknown origin after aortic root transplantation. Four patients had clinically active osteomyelitis with scintigraphic evidence of migration of labeled granulocytes. In all 26 patients the PGP/TBGP values were calculated for $t = 15$ min and in 10 patients (2 with vasculitis, 2 bone marrow transplants, 2 with IBD, and 4 with osteomyelitis) also for $t = 30$ min.

In 19 of these 26 patients (4 controls, 4 with IBD, 4 with

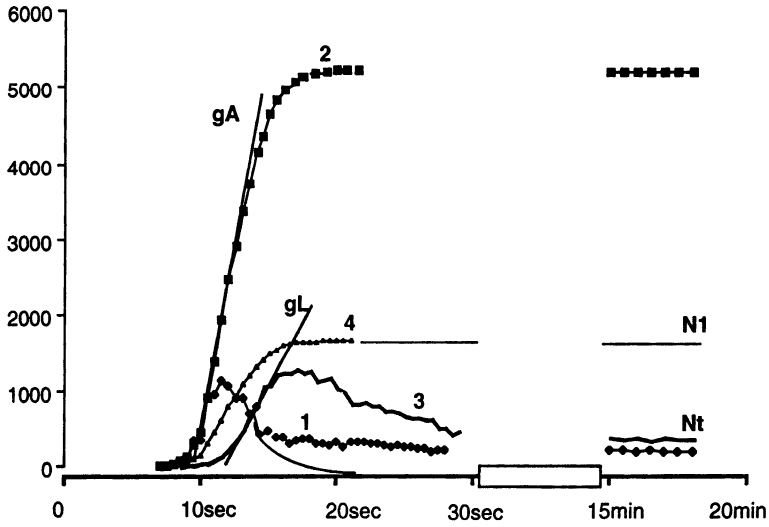

FIG. 1. Principle of technique for quantifying pulmonary vascular granulocyte pool. Time-activity curve (*curve 1*) recorded from input region of interest (ROI) has been integrated to produce *curve 2*. This is then scaled to be parallel to upslope of curve (*curve 3*) recorded from lung ROI to generate curve (*curve 4*) that represents curve that would have been obtained from lung if all injected labeled granulocytes had been trapped in lung on first pass. Scaling factor (see text for derivation) is ratio of upslope gradients gL and gA of *curves 3* and *2*, respectively. Actual lung curve (*curve 3*) decreases from initial peak as granulocytes enter and equilibrate within whole body marginating pools such that equilibrium count rate (N_t) in relation to plateau count rate (N_1) of *curve 4* is equal to ratio of pulmonary granulocyte pool (PGP) to total body granulocyte pool (TBGP).

vasculitis, 4 with osteomyelitis, 2 bone marrow recipients, and 1 renal transplant recipient), the R of labeled cells was determined as the percentage of injected cell-associated activity that was still circulating at a specific time (t) after injection. In all these patients, the PGP/CGP values were calculated using R values based on blood samples at t = 15 min and in 10 patients also at t = 30 min. The calculation of R was based on total blood volume estimated from the patient's weight and height (23) as R = (1 ml sample radioactivity × total blood volume)/injected activity. R was calculated without any further cell purification because the cells were isolated in pure form before labeling.

Cell Labeling

Granulocytes were isolated from 100 ml of fresh acid-citrate dextrose (formula A) anticoagulated blood by plasma-Percoll gradient centrifugation and labeled with ^{99m}Tc, as described previously (33). The mean efficiency of cell labeling was 54 ± 12% (SD).

Imaging and Data Analysis

^{99m}Tc-MAA and ^{99m}Tc-granulocyte dual studies. A small dose of ^{99m}Tc-labeled MAA (13–15 MBq) was first injected intravenously, and a posterior planar lung scan was acquired for 5 min. The ^{99m}Tc-labeled granulocytes were then injected as a bolus via a different butterfly cannula, and a dynamic first-pass study was acquired in a 64 × 64-pixel matrix at a sequence of 120 × 1-s frames for 2 min and 30 × 30-s frames for up to 17 min after injection. The total amount of radioactivity injected as ^{99m}Tc-granulocytes was 157 ± 19 MBq. The radioactivity doses of both injections were precisely determined using a well counter before and after injection. All injections were made with patients in the supine position.

ROIs were placed over the superior vena cava, right ventricle, pulmonary artery, and peripheral regions of the lung (right midzone) at about the level of the pulmonary artery. Time-activity curves were generated and calculations were performed by using the theory described above.

The count rate in the lung ROIs in the ^{99m}Tc-MAA image was recorded. A time-activity curve was then generated in the same lung ROI from the ^{99m}Tc-granulocyte dynamic first-pass study after the background due to the previously injected Tc-MAA had been subtracted. Arterial input time-activity curves were generated from the ROIs over the superior vena cava, right ventricle, and pulmonary artery. Recirculation of the labeled cells was corrected by using a monoexponential approximation for the descending shoulder of the curve, and the areas under the corrected curves were obtained by integration. The total available dose of ^{99m}Tc-labeled granulocytes was calculated for the lung ROI, by the method described above, as the integral under the first-pass arterial input time-activity curve made parallel to the lung curve (Fig. 1) separately for the three different arterial input curves.

^{99m}Tc-MAA lung scans and ^{99m}Tc-labeled granulocyte first-pass studies were acquired using a conventional large field-of-view gamma camera (Starcam, General Electric) placed posteriorly to the thorax as near as possible to the patient's chest and on-line to a dedicated computer (Starimager, General Electric).

The assumption that the vertical distributions of ^{99m}Tc-MAA and ^{99m}Tc-granulocytes are equal was tested as follows. Vertical profiles were drawn over the middle of the right lung for the ^{99m}Tc-MAA static image and the 15-min frame of the dynamic ^{99m}Tc-granulocyte study (corrected for the ^{99m}Tc-MAA background). The granulocyte profile was then divided by the ^{99m}Tc-MAA profile. If the regional blood flow and regional PGP are similar, the ratio of ^{99m}Tc-granulocyte and ^{99m}Tc-MAA profiles should remain constant over the lung, with a correlation coefficient between the ratio and distance to diaphragm statistically not different from zero.

The study was approved by the Ethics Committee of the Hammersmith Hospital and by the Administration of Radioactive Substances Advisory Committee (UK). Informed written consent was obtained from each person referred for the study.

Application to patients. The same analytical computational approach was adopted for the measurement of PGP in the 26 patients described above not given ^{99m}Tc-MAA. Radioactivity in the injection syringe was measured before and after injection for the calculation of R. The lung ROI was placed in the midzone of the right lung. Subsequent images were obtained at 15 min (in all 26 patients) and 30 min (in 10 patients). In most patients, blood samples were also taken at these times: in 19 patients at 15 min and in 10 patients at both times.

RESULTS

Validation of the First-Pass Integration Technique

The correlation coefficient of the least squares fit, either to the integrated input curve or to the lung curve,

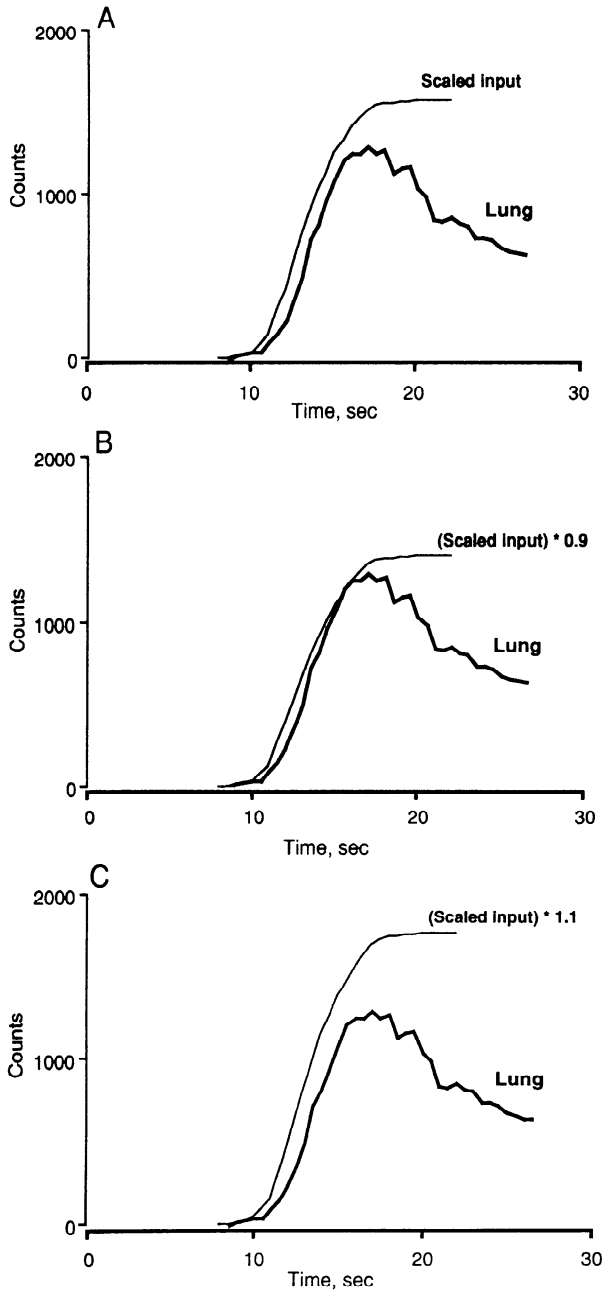

FIG. 2. *A*: objective derivation of gL/gA. Scaled integrated input curve is compared with recorded lung curve after scaling based on least squares regression fits to 6 or 7 points on respective upslope segments. *B* and *C*: subjective derivation of gL/gA. Same comparison is shown except objectively scaled input curve has been changed by +10% (*B*) and −10% (*C*). The 2 scaled input curves are now clearly not parallel to the lung curve.

was not <0.94 ($n > 6$), with a mean of 0.986 ± 0.012 for gA and 0.973 ± 0.015 for gL. The factor by which the integrated input curve was scaled was essentially the same for the operator-independent and visual approaches ($r = 0.98$; $P < 0.0002$). The effect of varying the scaling factor by 10% is shown in Fig. 2.

Comparison of the ratios of the doses of the radiopharmaceuticals measured in vitro with the ratio of in vivo lung ROI count rates measured by the computerized objective method are presented in Fig. 3 for the superior vena cava, right ventricle, and pulmonary artery ROIs, respectively. All three ROIs gave mean values close to unity: 0.98 ± 0.079 for the superior vena cava, 1.01 ± 0.070 for the right ventricle, and 0.97 ± 0.073 for the pulmonary artery. All these arterial input ROI values did not differ significantly in any pair comparison ($P > 0.1$ for all). Thus there is no evidence to suggest that any of these ROIs is preferable, and the advantage of any particular one depends on technical considerations and the ease of localization of the vascular structures in a given patient. The right ventricular ROI was generally the easiest to visualize and was used to quantify the arterial input time-activity curve in the subsequent patient studies.

Comparison of ^{99m}Tc-Granulocyte and ^{99m}Tc-MAA Profiles

The relationship between ^{99m}Tc-granulocyte and ^{99m}Tc-MAA profiles is presented in Fig. 4. It is clear that the segment of the ratio curve corresponding to the lung is constant. A subdiaphragmatic peak, where an MAA signal is absent, and a smaller "noisy" one above the apex, corresponding to clavicular bone marrow where MAA is again absent, can be identified. In no patient was the correlation coefficient between the ^{99m}Tc-granulocyte-to-^{99m}Tc-MAA ratio and the distance to diaphragm >0.004 [mean (±SD) value 0.0026 ± 0.0018].

PGP Expressed in Terms of TBGP

The ^{99m}Tc-granulocyte pulmonary vascular pool was calculated as the ratio PGP/TBGP at 15 min ($n = 26$) and at 30 min ($n = 10$) after injection. The values of PGP/TBGP are summarized in Fig. 5. The values of PGP/TBGP at 15 and 30 min were very similar. At 15 min, the mean value in patients with IBD of PGP/TBGP was 0.22 ± 0.07 ($n = 7$), almost three times

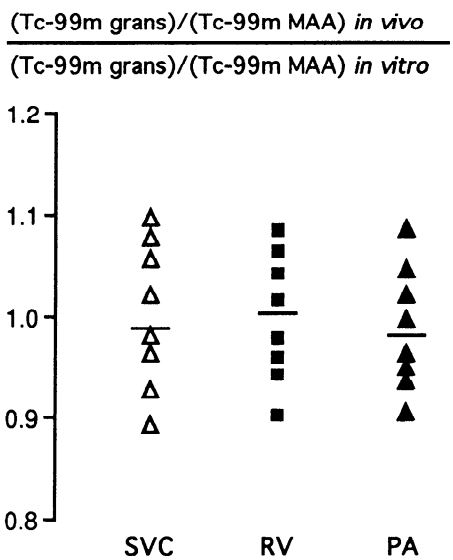

FIG. 3. Ratios of count rate (N_1) to count rate given by a preceding dose of ^{99m}Tc-macroaggregated albumin (MAA) after correction for respective injected doses given by 3 different input ROIs: superior vena cava (SVC), right ventricle (RV), and pulmonary artery (PA). grans, Granulocytes. Horizontal lines, means.

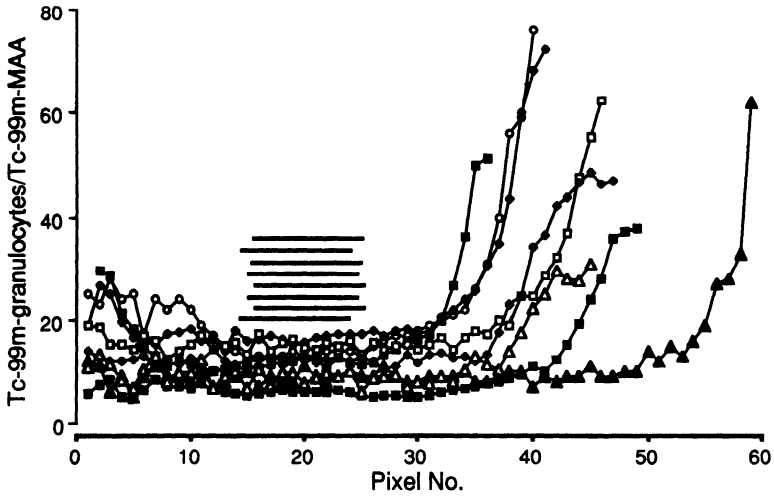

FIG. 4. Ratio of vertical (apex to base) lung ^{99m}Tc-granulocyte and ^{99m}Tc-MAA profile curves as a function of distance from right lung apex. Different symbols represent different subjects. Horizontal bars, vertical distances of ROIs placed over lung in each subject.

higher than in the control group (0.08 ± 0.01; $P < 0.005$; $n = 5$). The mean value in patients with vasculitis was 0.34 ± 0.07; $n = 5$), also significantly higher compared with the control group ($P < 0.001$). Patients with posttransplant inflammatory conditions had a mean PGP/TBGP of 0.33 ± 0.08 ($P < 0.01$; $n = 5$) and patients with osteomyelitis had a mean of 0.15 ± 0.06 ($P > 0.1$; $n = 4$).

There was no difference in PGP/TBGP between 15 and 30 min either in patients with extensive systemic inflammatory conditions (PGP/TBGP = 0.33 ± 0.02 at 15 min and 0.32 ± 0.02 at 30 min; $P > 0.1$; $n = 10$) or in patients with osteomyelitis (0.15 ± 0.06 at 15 min and 0.14 ± 0.03 at 30 min; $P > 0.1$; $n = 4$).

PGP Expressed in Terms of CGP

If we assume that granulocytes temporarily retained in the pulmonary vessels are exchanging with the peripheral blood circulating pool, it is physiologically valid to quantify the PGP as a fraction of the CGP, i.e., as PGP/(TBGP × R). This measurement was performed in 19 patients, and the data are presented in Fig. 6. The mean values of PGP/CGP at 15 min after injection were 0.24 ± 0.03 for control patients ($n = 4$), 0.92 ± 0.10 for patients with IBD ($n = 4$; $P < 0.01$ compared with control patients), 1.12 ± 0.38 for patients with vasculitis ($n = 4$; $P < 0.05$ compared with control patients), 0.96 ± 0.30 for transplant recipients ($n = 3$; $P < 0.05$ compared with control patients) and 0.54 ± 0.20 for patients with osteomyelitis ($n = 4$; $P < 0.05$ compared with control patients).

Similar to PGP/TBGP, PGP expressed as a fraction of CGP did not differ significantly between 15 and 30 min. In particular, PGP/CGP in patients with extensive inflammatory disease was 1.15 ± 0.30 at 15 min and 1.18 ± 0.32 at 30 min ($n = 6$; $P > 0.1$) and in patients with osteomyelitis it was 0.54 ± 0.20 at 15 min and 0.49 ± 0.13 at 30 min ($n = 4$; $P > 0.1$).

DISCUSSION

Quantification of PGP

Quantification of the PGP has previously been based on the measurement of the half-time of the pulmonary

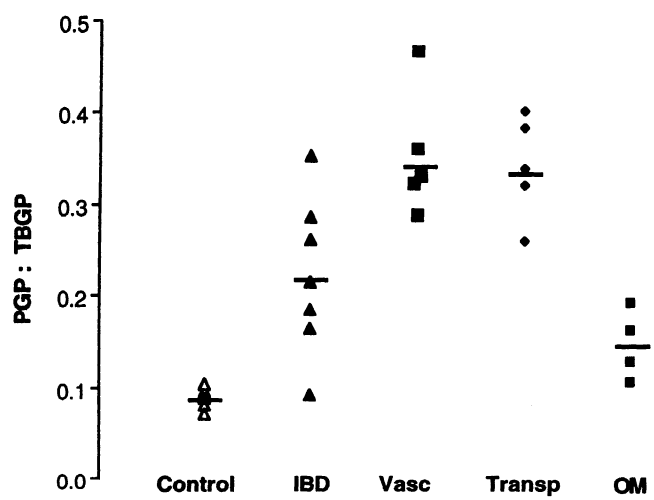

FIG. 5. Ratio of PGP to TBGP measured 15 min after injection of ^{99m}Tc-hexamethylpropyleneamine oxime-labeled granulocytes in control subjects, transplant recipients (transp), and patients with inflammatory bowel disease (IBD), systemic vasculitis (vasc), and osteomyelitis (OM). Horizontal lines, means.

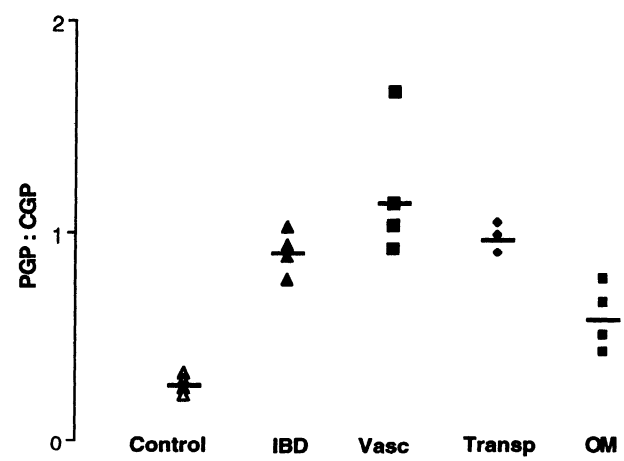

FIG. 6. Ratio of PGP to circulating granulocyte pool (CGP) measured 15 min after injection of ^{99m}Tc-HMPAO-labeled granulocytes in control subjects, transplant recipients (transp), and patients with IBD, vasc, and OM. Horizontal lines, means.

disappearance of labeled cells (45) as the ratio of chest to whole body radioactivity using gamma camera whole body scans (4), as the lung-to-liver count ratio (20), and, more precisely, as the mean transit time through the pulmonary vascular bed (24, 28, 34). These techniques have several drawbacks. The half-time of disappearance (45) is physiologically indefinable and will, to some extent, depend on the disappearance rate of labeled granulocytes from the blood. The first-pass techniques may be influenced by artifactual lung sequestration of granulocytes activated or damaged during the labeling procedure. The technique originally described by MacNee et al. (24) and Muir et al. (29), involving the integration of the lung curve instead of the input curve, was difficult to justify theoretically and has recently been modified on experimental grounds (19), although the new technique, which defines granulocyte retention from the respective peaks of the left ventricular time-activity curves recorded after separate injection of labeled red blood cells and granulocytes, is also theoretically doubtful because of the different pulmonary transit times of the two cells and the resulting different shapes of the two curves. The expression of PGP as a quotient of the transit times of granulocytes and red blood cells is appealing because it separates the pulmonary marginating pool from the pulmonary circulating pool (combined in the current technique as the PGP), but the method requires the use of a separate red blood cell label.

All of these methods, including the current one but not including the first-pass technique of MacNee et al. (24), are subject to errors resulting from bone marrow accumulation of activity in the bone marrow of the chest wall. The bone marrow marginates granulocytes and is therefore visible even on early labeled granulocyte scans. It is more prominent on late scans (2, 36) as a result of the destruction of labeled cells (26). Thus, overlapping bone marrow in ribs could be a potential source of error in pulmonary granulocyte kinetic quantification with respect to dynamic studies as well as delayed (i.e., 24 h) static imaging. In addition, there may be different gravity-dependent variations of pulmonary blood flow and granulocyte mean transit time (24). To minimize this effect, we placed the lung ROI at the midthoracic level, the same level as the arterial input ROI. Nevertheless, the vertical distributions of regional PGP and regional blood flow were shown in our study to be very similar in patients without evidence of local lung inflammation.

The numerical approach applied here for the estimation of the lung curve that would be obtained if all the injected granulocytes were trapped has been used for quantitative ^{99m}Tc-diethylenetriamine pentaacetic acid studies of kidney perfusion and function (31, 32). The three different ROIs gave equivalent integrated arterial input data. The 10% statistical error could be caused by factors such as the superimposition of overlying pulmonary tissue and the difficulty of drawing an ROI over the pulmonary artery separately from adjacent heart chambers and pulmonary tissue. Bolus injection technique and bolus volumes may be another factor (3). We injected a small-volume bolus (<2 ml) and then rapidly flushed with 20 ml of saline, a technique that is commonly approved as the best for bolus injection.

The measurement of PGP/TBGP assumes that the labeled cells have equilibrated throughout their marginating pools by the time the count rate in the lung ROI is determined for comparison with the first-pass count rate. Although 15 min may, in theory, be too early for equilibration, there was no significant difference between the values of PGP/TBGP based on lung counts at 15 and 30 min, respectively.

PGP in Disease

There is a significant difference between PGP values obtained in control individuals and patients with different systemic inflammatory diseases. It is known from microscopic measurements that the cross-sectional diameter of pulmonary capillaries is significantly smaller than those of granulocytes (38), and therefore the granulocyte has to undergo distortion while passing through the lung capillary network (5). Under such conditions, the shape change properties, particularly mechanical stiffness, are important determinants of capillary granulocyte passage velocity, as demonstrated in vitro (1) and in vivo (6, 17). Mechanical stiffness of the granulocyte membrane itself depends on a number of Ca^{2+}-mediated cellular mechanisms, especially the actions of C5a and *N*-formylmethionyl-leucyl-phenylalanine (28, 39, 49) as well as interleukins-1 and -2 (8, 9). Increased granulocyte activation, mediated through all these pathophysiological mechanisms, has been shown in patients with active IBD by using microscopic shape change methods (27). An activated granulocyte demonstrates an increased stiffness and delayed speed of passage through the glass microcapillary (1, 7) as the increased activation directly relates to mechanical stiffness of the cell (9, 10). Our data can most easily be explained as the in vivo expression of the same pathophysiological processes because the pulmonary capillaries have roughly the same space relationships to granulocytes as in the in vitro experiments mentioned above (18).

Another pathophysiological mechanism likely to promote an increase in the pulmonary vascular pool of labeled granulocytes is the activation of the lung vascular endothelium that results in enhanced adhesiveness of the endothelium to circulating cells (15). This has been described, particularly in systemic (42) and abdominal (14) inflammation, due to expression of endothelial adhesion molecules on the pulmonary endothelial cell surface in response to cytokines generated locally at the site of inflammation (12, 41).

Theoretically, the cell could be activated by the labeling technique itself (37). In our patients, all the labeling procedures were performed exclusively in plasma, which is generally accepted as resulting in a minimal degree of cell activation and damage (16). Absence of the typical pattern of cell kinetics described for in vitro activation (37), namely, immediate increased lung sequestration with early clearance and subsequent redistribution of cells to the liver, is a strong argument

against the in vitro activation of granulocytes. It should be appreciated that even if some level of "labeling injury" had been present during the first pass, as opposed to subsequent passes (30, 37), it would not affect the calculation of PGP because the first-pass data in this technique serve only to calibrate the injected dose in relation to the first-pass count rate in the lung ROI. Studies of the relationship between activation status at the time of injection and the PGP are now in progress.

In conclusion, increased intravascular pooling of granulocytes may be a prerequisite for granulocyte migration into the lung parenchyma and subsequent lung damage but, by itself, is unlikely to cause damage. This hypothesis is in line with the experimental findings of Henson's group (22, 46), who demonstrated intravascular neutrophil accumulation without evidence of extravascular migration histologically after systemic complement activation. The technique described here has the potential to quantify pulmonary vascular granulocyte pooling in clinical lung disease and, in conjunction with techniques for quantifying granulocyte migration (43), may help to define the respective roles of margination and migration in causing lung damage. Such studies using granulocytes double labeled with ^{99m}Tc (to measure margination) and ^{111}In (to measure migration) (44) are currently underway.

We are grateful to D. Bradley for expert radiographic assistance. W. Y. Ussov is supported by The Wellcome Trust.

Address for reprint requests: A. M. Peters, Dept. of Radiology, Hammersmith Hospital, Du Cane Road, London W12 0HS, UK.

Received 10 January 1994; accepted in final form 19 October 1994.

REFERENCES

1. **Armstrong, M., Jr., D. Needham, D. L. Hatchell, and R. S. Nunn.** Effect of pentoxifylline on the flow of polymorphonuclear leukocytes through a model capillary. *Angiology* 41: 253–262, 1990.
2. **Axelsson, B., B. Kalin, S. von Kruisensterna, and H. Jacobson.** Comparison of In-111 granulocytes and Tc-99m albumin colloid for bone marrow scintigraphy by use of quantitative SPECT Imaging. *Clin. Nucl. Med.* 15: 473–479, 1990.
3. **Bell, S. D., and A. M. Peters.** Blood flow measurment from first pass time/activity curves: influence of bolus spreading. *Nucl. Med. Commun.* 11: 477–480, 1990.
4. **Bureau, M. F., E. Malanchere, M. Pretolani, M. A. Boukili, and B. B. Vargaftig.** A new method to evaluate extravascular albumin and blood cell accumulation in the lung. *J. Appl. Physiol.* 67: 1479–1488, 1989.
5. **Chien, S., G. W. Schmid-Schoenbein, K. L. P Sung, E. A. Schmalzer, and R. Skalak.** Viscoelastic properties of leucocytes. In: *White Cell Mechanics: Basic Science and Clinical Aspects,* edited by H. J. Meiselman, M. A. Lichtlen, and P. L. LaCelle. New York: Liss, 1984, p. 19–51
6. **Doerschuk, C. M., N. Beyers, H. O. Coxson, B. Wiggs, and J. C. Hogg.** Comparison of neutrophil and capillary diameters and their relation to neutrophil sequestration in the lung. *J. Appl. Physiol.* 74: 3040–3045, 1993.
7. **Downey, G. P., and G. S. Worthen.** Neutrophil retention in the model microcapillaries: deformability, geometry, and hydrodynamic forces. *J. Appl. Physiol.* 65: 1861–1871, 1988
8. **Ferrante, A.** Activation of neutrophils by interleukins-1 and -2 and tumor necrosis factors. *Immunol. Ser.* 57: 417–436, 1992.
9. **Frank, R. S.** Time-dependent alterations in the deformability of human neutrophils in response to chemotactic activation. *Blood* 76: 2606–2612, 1990.
10. **Freyburger, G., F. Belloc, and M. R. Boisseau.** Pentoxifylline inhibits actin polymerization in human neutrophils after stimulation by chemoattractant factor. *Agents Actions* 31: 72–78, 1990.
11. **Gadek, J. E.** Adverse effects of neutrophils on the lung. *Am. J. Med.* 92: 27S–31S, 1992.
12. **Gross, V., T. Andus, H. G. Leser, M. Roth, and J. Scholmerich.** Inflammatory mediators in chronic inflammatory bowel diseases. *Klin. Wochenschr.* 21–23: 981–987, 1991.
13. **Guice, K. S., K. T. Oldham, M. G. Caty, K. J. Johnson, and P. A. Ward.** Neutrophil-dependent oxygen radical-mediated lung injury associated with acute pancreatitis. *Ann. Surg.* 206: 740–747, 1989.
14. **Hansson, L., J. Thorne, and B. Jeppsson.** Reduced clearance of leukocytes from lungs in septic rats. *Res. Exp. Med.* 192: 197–204, 1992.
15. **Harlan, J. M.** Leucocyte-endothelial interactions. *Blood* 65: 513–525, 1985.
16. **Haslett, C., L. A. Guthrie, M. M. Kopaniak, R. B. Johnston, and P. M. Henson.** Modulation of the multiple neutrophil functions by preparative methods of trace concentrations of bacterial lipopolysaccharide. *Am. J. Pathol.* 119: 101–110, 1985.
17. **Hill, H. R., N. H. Augustine, J. A. Newton, A. O. Shigeoka, E. Morris, and F. Sacchi.** Correction of developmental defect in neutrophil activation and movement. *Am. J. Pathol.* 128: 307–314, 1987.
18. **Hogg, J.** Neutrophil kinetics and lung injury. *Physiol. Rev.* 67: 1249–1295, 1987.
19. **Hogg, J. C., C. M. Doerschuk, B. Wiggs, and D. Minshall.** Neutrophil retention during a single transit through the pulmonary circulation. *J. Appl. Physiol.* 73: 1683–1685, 1992.
20. **Jonker, N. D., A. M. Peters, M. Carpani de Caski, H. J. Hodgson, and J. P. Lavender.** Pulmonary granulocyte margination is increased in patients with inflammatory bowel disease. *Nucl. Med. Commun.* 13: 806–810, 1992.
21. **Jonker, N. D, A. M. Peters, G. Gaskin, C. D. Pusey, and J. P. Lavender.** A retrospective study of radiolabeled granulocyte kinetics in patients with systemic vasculitis. *J. Nucl. Med.* 33: 491–497, 1992.
22. **Larsen, G. S., R., O. Webster, G. S. Worthen, R. S. Gumbay, and P. M. Henson.** Additive effect of intravascular complement activation and brief episodes of hypoxia in producing increased permeability in the rabbit lung. *J. Clin. Invest.* 75: 902–910, 1982.
23. **Lewis, S. M., and J. A. Liu Yin.** Blood volume studies. In: *Radionuclides in Haematology,* edited by S. M. Lewis and R. J. Bayley. Edinburgh: Churchill-Livingstone, 1986, p. 198–213.
24. **MacNee, W., B. A. Martin, B. R. Wiggs, A. S. Belzberg, and J. C. Hogg.** Regional pulmonary transit times in humans. *J. Appl. Physiol.* 66: 844–850, 1989.
25. **MacNee, W., and C. Selby.** Neutrophil kinetics in the lungs. *Clin. Sci. Lond.* 79: 97–107, 1990.
26. **Mant, M. J., P. A. Gordon, and J. J. Akabutu.** Bone marrow granulocyte reserve in chronic benign idiopathic neutropenia. *Clin. Lab. Haematol.* 9: 281–288, 1987.
27. **McCarthy, D. A., D. S. Rampton, and Y. C. Liu.** Peripheral blood neutrophils in inflammatory bowel disease: morphological evidence of in vivo activation in active disease. *Clin. Exp. Immunol.* 86: 489–93, 1991.
28. **Mrowietz, U., J. M. Schroeder, J. Brasch, and E. Christophers.** Infiltrating neutrophils differ from circulating neutrophils when stimulated with C5a, NAP-1/IL-8, LTB4 and FMLP. *Scand. J. Immunol.* 35: 71–78, 1992.
29. **Muir, A. L., M. Cruz, B. A. Martin, H. V. Thomassen, A. Belzberg, and J. C. Hogg.** Leucocyte kinetics in the human lung: role of exercise and catecholamines. *J. Appl. Physiol.* 57: 11–19, 1984.
30. **Peters, A. M., P. Allsop, A. W. J. Stuttle, R. N. Arnot, M. Gwilliam, and G. M. Hall.** Granulocyte margination in the human lung and its response to the strenous exercise. *Clin. Sci. Lond.* 82: 237–244, 1992.
31. **Peters, A. M., J. Brown, G. G. Hartnell, M. J. Myers, C. Haskell, and J. P. Lavender.** Non-invasive measurement of renal blood flow with 99mTc-DTPA: comparison with radiolabelled microspheres. *Cardiovasc. Res.* 21: 830–834, 1987.
32. **Peters, A. M., R. D. Gunasekera, J. P. Lavender, M. J. Myers, I. Gordon, J. M. Ash, and D. L. Gilday.** Noninvasive

measurement of renal blood flow using DTPA. *Contrib. Nephrol.* 56: 26–30, 1987.

33. **Peters, A. M., M. E. Roddie, H. J. Danpure, S. Osman, G. P. Zacharopoulos, P. George, A. W. J. Stuttle, and J. P. Lavender.** Tc-99m-HMPAO labelled leucocytes: comparison with In-111 labelled granulocytes. *Nucl. Med. Commun.* 19: 449–463, 1988.
34. **Peters, A. M., S. H. Saverymuttu, R. N. Bell, and J. P. Lavender.** Quantification of the distribution of the marginating granulocyte pool in man. *Scand. J. Haematol.* 34: 111–120, 1985.
35. **Peters, A. M., S. H. Saverymuttu, A. Keshavarzian, R. N. Bell, and J. P. Lavender.** Splenic pooling of granulocytes. *Clin. Sci. Lond.* 68: 283–289, 1985.
36. **Peters, A. M., S. H. Saverymuttu, H. J. Reavy, H. J. Danpure, S. Osman, and J. P. Lavender.** Imaging of inflammation with indium-111 tropolonate labeled leukocytes. *J. Nucl. Med.* 24: 39–44, 1983.
37. **Saverymuttu, S. H., A. M. Peters, H. J. Danpure, H. J. Reavy, S. Osman, and J. P. Lavender.** Lung transit of 111Indium-labelled granulocytes. Relationship to labelling techniques. *Scand. J. Haematol.* 30: 151–160, 1983.
38. **Schmid-Schoenbein, G. W., Y. Y. Shik, and S. Chien.** Morphometry of human leucocytes. *Blood* 56: 866–875, 1980.
39. **Sullivan, G. W., H. T. Carper, and G. L. Mandell.** Pentoxifilline modulates activation of human neutrophils by amphotericin B in vitro. *Antimicrob. Agents Chemother.* 36: 408–416, 1992.
40. **Tate, R. M., and J. E. Repine.** Neutrophils and the adult respiratory distress syndrome. *Am. Rev. Respir. Dis.* 128: 552–559, 1983.
41. **Thornhill, M. H., and D. O. Haskard.** IL-4 regulates endothelial cell activation by IL-1, tumor necrosis factor or IFN-gamma. *J. Immunol.* 145: 865–872, 1990.
42. **Traber, D. L., G. Schlag, H. Redl, W. Strohmair, and L. D. Traber.** Pulmonary microvascular changes during hyperdynamic sepsis in an ovine model. *Circ. Shock* 22: 185–193, 1987.
43. **Ussov, W. Y., A. M. Peters, H. J. F. Hodgson, and J. M. B. Hughes.** Quantification of pulmonary uptake of Indium-111 labelled granulocytes in inflammatory bowel disease. *Eur. J. Nucl. Med.* 21: 6–11, 1994.
44. **Ussov, W. Y., A. M. Peters, J. M. B. Hughes, D. M. Glass, G. Gaskin, A. Spencer, C. D. Pusey, and H. J. F. Hodgson.** Pulmonary vascular granulocyte kinetics and alveolocapillary barrier damage in extrapulmonary conditions (Abstract). *J. Nucl. Med.* 33, *Suppl.*: P132, 1994.
45. **Warshawsky, F. J., W. J. Sibbald, A. A. Driedger, and H. Cheung.** Abnormal neutrophil-pulmonary interactions in the adult respiratory distress syndrome. Qualitative and quantitative assessment of pulmonary neutrophil kinetics in humans with in vivo Indium-111 neutrophil scintigraphy. *Am. Rev. Respir. Dis.* 133: 797–804, 1986.
46. **Webster, R. O., G. S. Larsen, B. C. Mitchell, A. J. Goins, and P. M. Henson.** Absence of inflammatory lung injury in rabbits challenged intravascularly with complement-derived chemotactic factors. *Am. Rev. Respir. Dis.* 125: 335–340, 1982.
47. **Weiland, J. F., W. B. Davis, J. F. Holter, J. R. Mohammed, P. M. Dorinsky, and J. E. Gadek.** Lung neutrophils in the adult respiratory distress syndrome. Clinical and pathophysiological significance. *Am. Rev. Respir. Dis.* 133: 218–225, 1987.
48. **Worthen, G. S., C. Haslett, A. J. Rees, R. S. Gumbay, J. H. Henson, and P. M. Henson.** Neutrophil mediated pulmonary vascular injury. *Am. Rev. Respir. Dis.* 136: 19–28, 1987.
49. **Worthen, G. S., B. Schwab, E. L. Elson, and G. P. Downey.** Mechanism of stimulated neutrophils: cell stiffening induces retention in capillaries. *Science Wash. DC* 245: 183–186, 1989.